NANO EXPRESS

Controlled Synthesis of Monolayer Graphene Toward Transparent Flexible Conductive Film Application

Byeong-Joo Lee · Han-Young Yu · Goo-Hwan Jeong

Abstract We demonstrate the synthesis of monolayer graphene using thermal chemical vapor deposition and successive transfer onto arbitrary substrates toward transparent flexible conductive film application. We used electron-beam-deposited Ni thin film as a synthetic catalyst and introduced a gas mixture consisting of methane and hydrogen. To optimize the synthesis condition, we investigated the effects of synthetic temperature and cooling rate in the ranges of 850–1,000°C and 2–8°C/min, respectively. It was found that a cooling rate of 4°C/min after 1,000°C synthesis is the most effective condition for monolayer graphene production. We also successfully transferred as-synthesized graphene films to arbitrary substrates such as silicon-dioxide-coated wafers, glass, and polyethylene terephthalate sheets to develop transparent, flexible, and conductive film application.

Introduction

Graphene is a newly discovered carbon-based monolayer sheet consisting of honeycomb structures with two-dimensional arrays [1]. It has been attracting great attention owing to its fascinating mechanical, electronic, and optical properties [1–3]. Fundamental and application research is being carried out intensively in order to determine the potential uses. Several approaches to synthesizing graphene have been developed, including mechanical and chemical exfoliation, thermal chemical vapor deposition (TCVD), the graphitization of silicon carbide, and the reduction of graphene oxides [4–8].

The TCVD method is considered an appropriate method for the large area synthesis of graphene [5, 9]. However, there is still a definite need for high-quality graphene production that also yields large area thickness uniformity. In addition, the synthesis mechanism remains poorly understood and requires further study [9, 10]. In terms of the industrial application aspects, its outstanding electrical conductivity in a plane and high elasticity makes graphene a powerful candidate material not only for various functional devices such as sensors and electronic elements but also for transparent flexible conductive (TFC) electrodes that can replace indium tin oxide film and therefore be used in flexible display, touch screens and flexible solar cells via transfer onto flexible and transparent receiving substrates [11]. In this context, a large area synthesis with high thickness uniformity and successful transfer ability are essential and urgent topics in the realization of the aforementioned applications.

Here, we demonstrate the optimization of monolayer graphene synthesis using TCVD and the subsequent transfer onto arbitrary substrates toward TFC film application. We mainly investigated the effects of synthetic temperature and cooling rate on graphene thickness. We found that synthesis at 1,000°C and a cooling rate of 4°C/min was the most effective combination for monolayer graphene production. We also successfully transferred

B.-J. Lee · G.-H. Jeong (✉)
Department of Advanced Materials Science and Engineering,
Kangwon National University, Chuncheon,
Gangwon-do 200-701, Korea
e-mail: ghjeong@kangwon.ac.kr

H.-Y. Yu
Electronics and Telecommunications Research Institute,
Daejeon 305-600, Korea

as-synthesized graphene films onto arbitrary substrates such as silicon-dioxide-covered wafers, glass, and polyethylene terephthalate (PET) polymer sheets for further development as TFC films.

Experimental Details

As a graphene synthesis substrate, Ni thin films (300 nm thickness) were deposited by electron-beam evaporation using a SiO_2-covered Si wafer. The substrate was cut to 2 cm × 2 cm in size and installed in a 1-inch quartz tube furnace, as shown in Fig. 1. The tube was evacuated using a mechanical pump and then filled with Ar gas until atmospheric pressure was reached. While heating to the synthesis temperature range of 850–1,000°C, a mixture of H_2 (500 sccm) and Ar (500 sccm) gas was used under ambient pressure. The heating rate was 20°C/min. After the synthesis temperature was reached, we held it 30-min further to stabilize the furnace and to obtain a single-crystalline Ni phase, as suggested in a previous report [12]. The gas was then promptly changed into a mixture consisting of CH_4 (5 sccm) and H_2 (1,500 sccm) that was flowed during the 10-min synthesis. The effect of cooling rate on the graphene microstructure was investigated by modulating the cooling rate to 2, 4, 6, and 8°C/min through intentional cooling using a fan.

Synthesized samples on a Ni catalytic layer were first examined using an optical microscope and an atomic force microscope (AFM, Park Systems XE-70). A representative optical microscopic image of as-grown samples at 1,000°C with a 4°C/min cooling rate is shown in Fig. 2a. We can distinguish the grain boundary of the Ni film and can also estimate the quality of graphene samples qualitatively since the thinner graphene region is light gray while the thicker regions are dark gray. In the AFM topographic image of the same sample (Fig. 2b), it was found that the grain boundary of the Ni film can be resolved and the partially folded region of the formed graphene sheet can be shown as linear lines with 3 nm height.
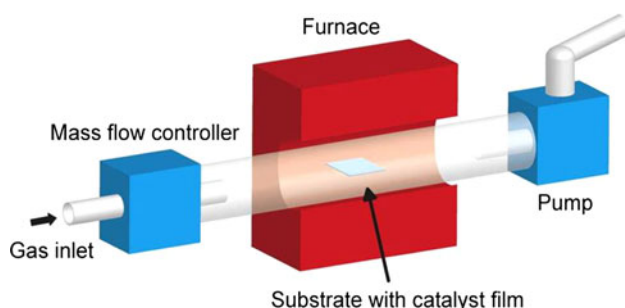
After synthesis, we performed graphene transfer to a SiO_2-covered Si wafer, glass plates, and PET sheets for further development. Here, we tried to carry out the transfer without a polymeric mediator such as polymethyl methacrylate film to prevent potential contamination during the removal of the polymeric films and thus preserve the clean surface of the as-synthesized graphene, as schematically shown in Fig. 2c. In brief, we first etched silicon dioxide using a 3M KOH solution at 75°C and obtained a catalytic Ni layer covered with graphene. The temperature of the solution was sensitive to removal of the SiO_2 layer. Then, we further etched out the Ni layer using a 1M $FeCl_3$ solution. When the Ni layer was completely removed, the graphene began floating on the solution and was discernable with the naked eye; we were thus able to scoop it up using receiving substrates. For optical microscopic observation, we used SiO_2 (300-nm thick)-coated Si wafers since we can clearly determine the number of graphene layers by color differences (Fig. 2d).
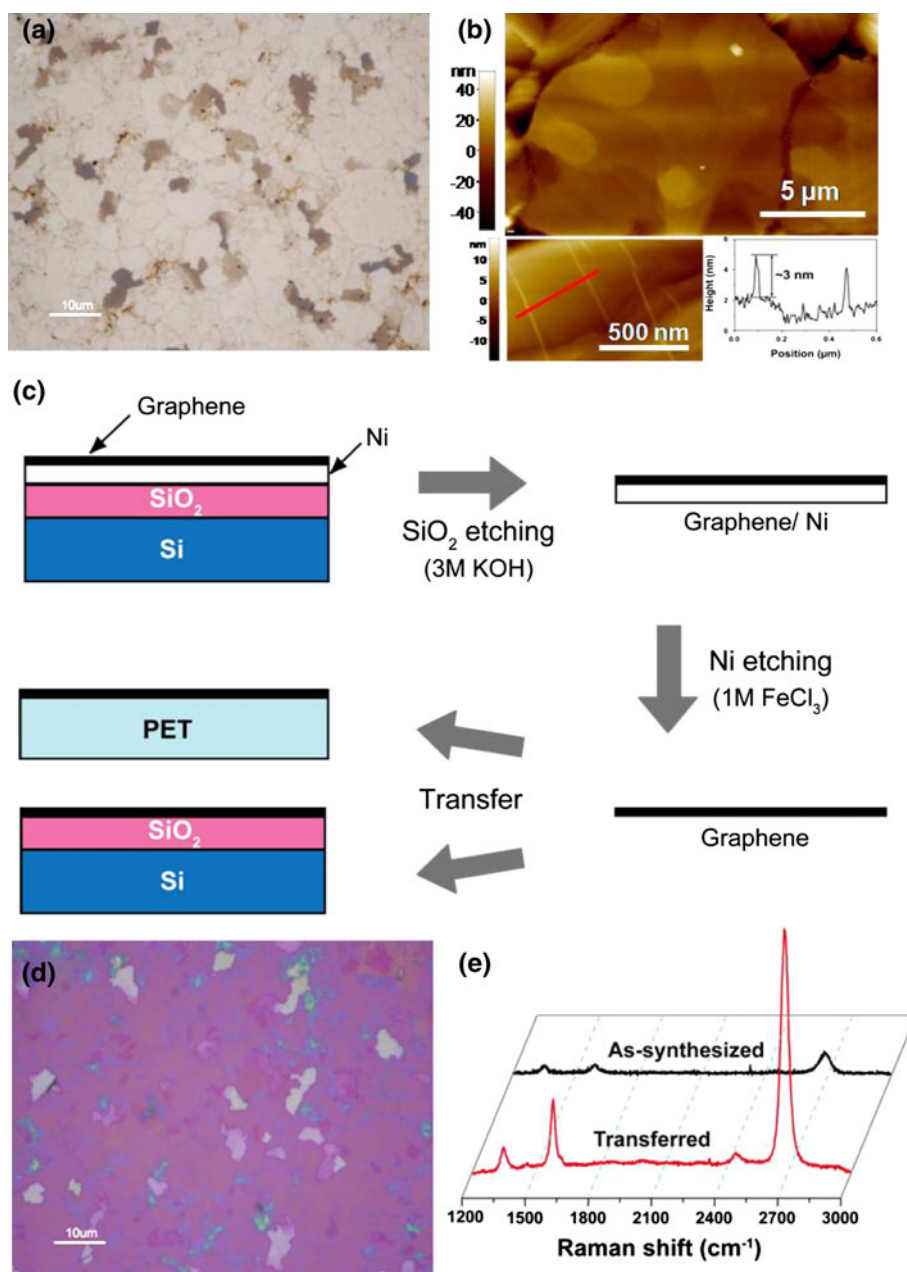
We were able to obtain enhanced Raman profiles after the transfer compared to the pristine samples on Ni films, as shown in Fig. 2e. Raman spectroscopy is a useful and convenient tool to examine the structural property of graphenes [13, 14]. Here, we used a 532-nm excitation wavelength laser with 1 μm spot size and low power of less 3 mW (Horiba Aramis). The Raman spectra ranges of 1,000–3,000 cm^{-1} from as-synthesized and transferred samples are comparatively shown in Fig. 2e. We obtained intensive peaks around 1,350, 1,600, and 2,700 cm^{-1}, which are known as the defect-induced D-band, the graphitic C–C vibration-related G-band, and the G′-band, which is an overtone of the D-band, respectively. In mono layer graphene, the G′-band shows a single Lorentzian profile below Raman frequency of 2,700 cm^{-1} and the intensity ratio of the G-band and the G′-band (IG/IG′) is below unity. As the number of graphene layers increases, the value of IG/IG′ decreases over unity and the line shape also becomes asymmetric.

Transmission electron microscopy (TEM, JEM2100 F) was used to reveal the detailed nanostructures of as-synthesized graphenes. The graphene samples for observation were prepared by direct transfer onto a TEM copper grid. For the characterization of the graphene-transferred-TFC film, the sheet resistance was measured by the four-point probe method, and transparency measurement was performed using incident light of 550-nm wavelength.

Results and Discussion

We first investigated the effect of synthesis temperature on the thickness uniformity of graphene; the results are shown in Fig. 3. The growth temperatures were 1,000, 900, and
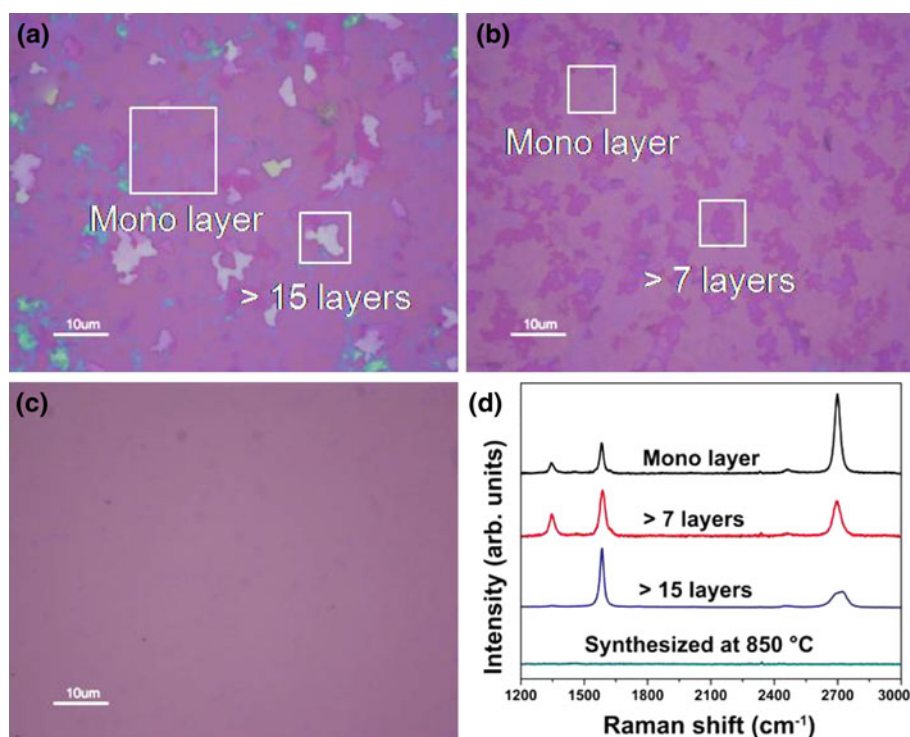

Fig. 1 Schematic illustration of a graphene synthesis system

Fig. 2 a Optical microscope image and **b** AFM topographic image of as-synthesized graphene on Ni catalytic films. Lower insets of (**b**) show graphene wrinkles on the substrate with 3 nm height. **c** Schematic presentation showing the graphene transfer without a polymeric mediator. **d** Optical microscope image of transferred graphene on a SiO₂-covered Si wafer. **e** Raman spectra show the intensity enhancement after the transfer

850°C; the optical images taken after transfer onto the SiO₂ wafer are given in Fig. 3a–c, respectively. As shown in Fig. 2d, we can easily distinguish monolayer graphene from the magenta color of the optical image, as indicated by the square in Fig. 3a. As the thickness of graphene increases, the color changes to purple as shown in Fig. 3b. The thickest area, which has more than 15 graphene layers, looks white, as shown in Fig. 3a. The estimation of graphene layers using optical images showed good concurrence with the results of Raman characterization, as shown in Fig. 3d. It was thus very useful to estimate the areal uniformity of the graphene samples with different growth parameters. The sample processed at 850°C had no

graphene over the substrate (Fig. 3c); this was also reconfirmed by the Raman analysis (Fig. 3d). On the basis of this result, it can be concluded that the synthetic temperature to produce graphene is a minimum of 900°C. It was found in the Raman spectra that the value of IG/IG′ decreases from 1.6 (>15 layers) to 0.86 (>7 layers) and 0.4 (monolayer) with the decrease in graphene layers. It is interesting to note that very thick graphene regions (>15 layers) are locally observed only in the 1,000°C samples although the areal coverage of monolayer graphene in the 1,000°C sample is higher than that of the 900°C sample. It is expected that the enhanced surface diffusion of carbon on Ni films in a 1,000°C environment gives rise to a locally

Fig. 3 Optical microscope images of synthesized graphenes at different temperatures: **a** 1,000°C, **b** 900°C, and **c** 850°C. **d** Raman spectra depend on the number of graphene layers in the samples

distributed very thick graphene region among the relatively large monolayer area when we take account of the graphene synthesis mechanism which is composed of feedstock dissolution, supersaturation, and precipitation of carbon on Ni catalysts [15]. In other words, insufficient carbon diffusion at 900°C results in relatively low areal monolayer coverage with moderate thickness as shown in Fig. 3b. We thus fixed the synthesis temperature at 1,000°C hereafter.

Next, we investigated the effect of cooling rate on the thickness uniformity of graphene since we expected that the carbon precipitation and diffusion on the Ni surface are critical to determining the number of graphene layers and large area synthesis. We fixed the synthesis temperature (1,000°C) and gas composition ($CH_4:H_2 = 5$ sccm: 1,500 sccm) so that we could ensure the same condition in the amount of carbon influx and decomposed carbon species. The cooling rate after the 1,000°C synthesis was changed to 8, 6, 4, and 2°C/min; their optical images are shown in Fig. 4a–d, respectively.

The optical image of the fastest cooled sample has very similar features as the 900°C-grown sample, which means that the carbon diffusion is insufficient, as shown in Fig. 4a. On the other hand, we can observe a mixture of monolayer and thick layer graphenes in the 6°C/min sample (Fig. 4b). The portion of thick graphene layer increased with decreasing cooling rate to 4°C/min (Fig. 4c), which implies that the enhanced surface diffusion of carbon might be responsible for the increased number of thick graphene spots through the Ostwald ripening phenomena in particle

agglomeration. However, with a very low cooling rate of 2°C/min, it seemed that the precipitated carbon was sufficiently diffused and finally made some carbonaceous compound along the grain boundary, as shown in Fig. 4d.

The aforementioned optical observation results were confirmed with the Raman results obtained from the representative area of each sample (Fig. 5a). We confirmed that the main products in the 8°C/min cooled sample are several layered graphenes and that monolayer graphene is formed in the 6 and 4°C/min cooling conditions. For the 2°C/min furnace-cooled sample, we did not observe graphite-related peaks.

We estimated the monolayer coverage based on the color difference of the optical images of Fig. 4. We also determined the value of the intensity ratio (IG/IG') from the Raman spectra (Fig. 5b). In brief, the areal coverage of graphene monolayer exceeds 75% in 6 and 4°C/min cooling samples while the 8°C/min cooled sample has approximately 26% areal coverage. In the Raman spectra analysis, the value of IG/IG' reaches 0.4, 0.8, and 1.6 with the increasing cooling rate of 4, 6, and 8°C/min, respectively. We can thus conclude from the results that the optimum temperature and cooling rate of our synthesis system is 1,000°C and 4°C/min, respectively. Figure 6 presents a representative highly magnified TEM image and electron diffraction pattern from the optimized sample. The bright field image shows a folded edge of monolayer graphene. The electron diffraction pattern shows hexagonally distributed several diffraction spots on polycrystalline

Fig. 4 Optical microscope images of synthesized graphenes with different cooling rates: **a** 8°C/min, **b** 6°C/min, **c** 4°C/min, and **d** 2°C/min
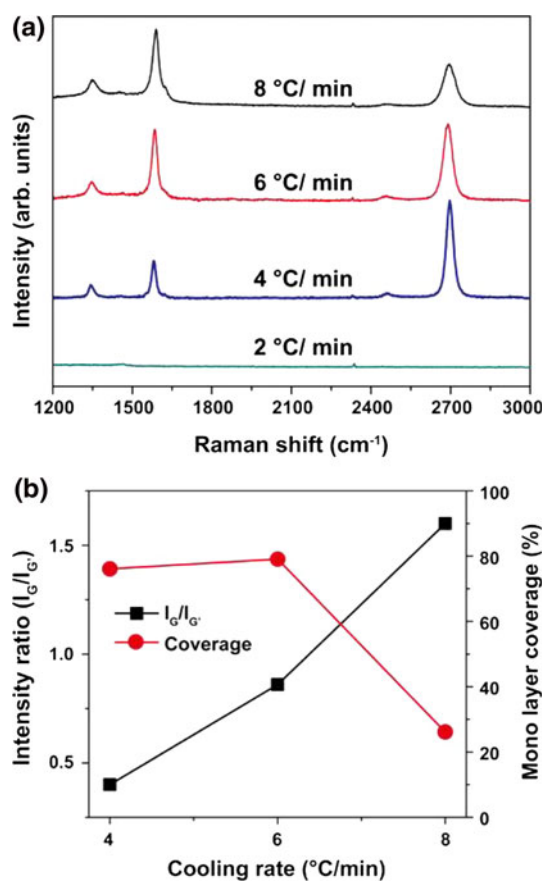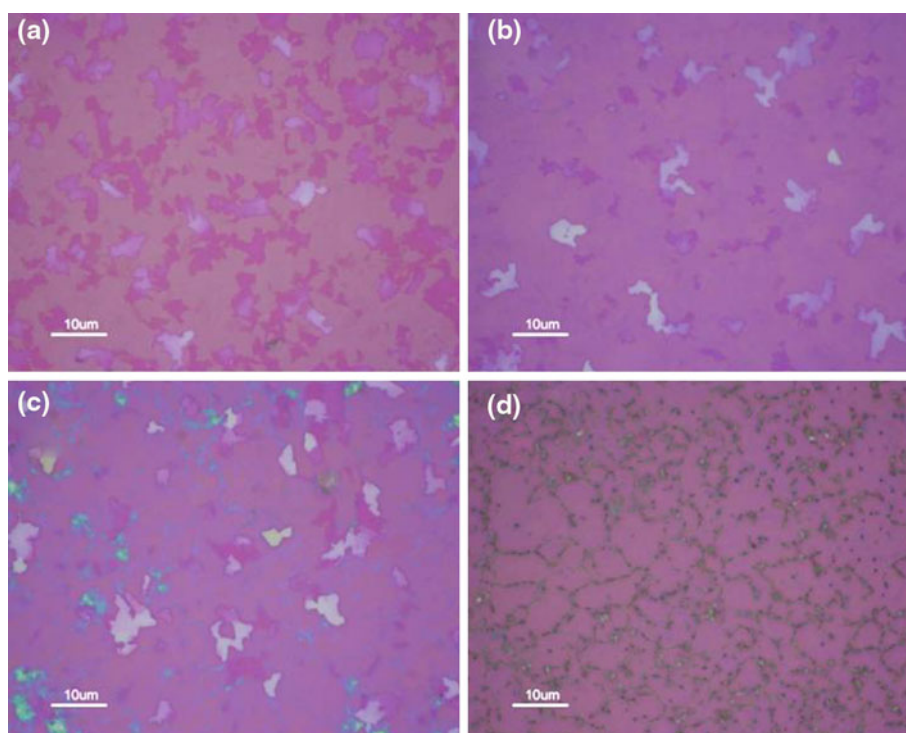

Fig. 5 a Raman spectra of synthesized graphenes with different cooling rates. **b** Effects of cooling rates on both peak intensity ratio ($I_G/I_{G'}$) and areal coverage of monolayer graphenes

ring, which means that the pattern is taken from few layered graphenes.

Finally, we fabricated transparent conductive film using the transfer technique of as-grown graphene in order to apply TFC films; the results are shown in Fig. 7. A transparency of 87% and sheet resistance of 1,540 Ω/sq. were obtained from the 4°C/min cooling sample presented as the left side inset in Fig. 7. The right inset is a digital camera image that shows the good conductivity of the transparent conducting graphene film. The transparency decreased to
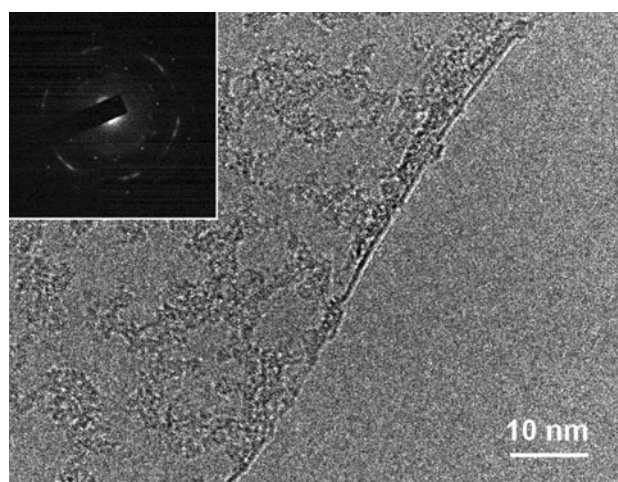

Fig. 6 a A representative TEM image of mono layer graphene synthesized at 1,000°C with a 4°C/min cooling rate. The *inset* shows the electron diffraction pattern of the sample
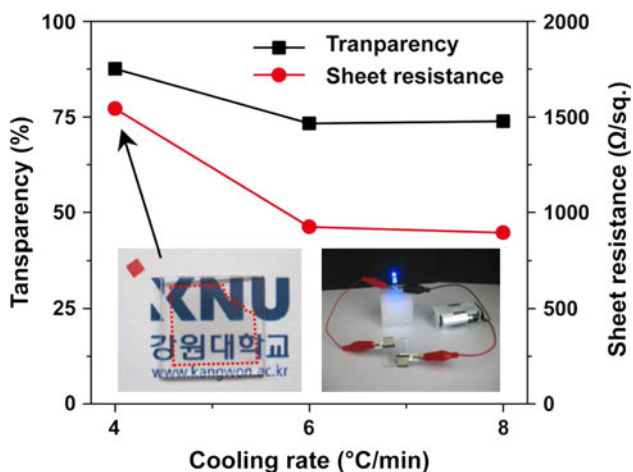
Fig. 7 Effects of cooling rates on sheet resistance and optical transmittance at the 550-nm wavelength of graphene-based TFC films. The *inset* shows a digital camera image of transferred graphene (*left*) and a demonstration of the illuminator (*right*)

73% and the sheet resistance also decreased to 890 Ω/sq. in the 8°C/min cooled sample. The reason for the decrease in the transparency and sheet resistance and the increase in the conductivity is the increased number of graphene layers with the increasing cooling rate. The transparency and conductivity are progressively being enhanced through further development of the system.

Conclusions

We demonstrated a growth optimization procedure for monolayer graphene using TCVD and its subsequent transfer onto various substrates toward TFC film application. We investigated the effects of synthetic temperature and cooling rate on graphene structures and found that synthesis at 1,000°C and a cooling rate of 4°C/min were the most effective conditions for monolayer graphene production. We also fabricated graphene-based TFC films via the transfer of as-grown graphene films onto PET or glass substrates without the use of polymeric mediators.

References

1. Y. Zhang, Y. Tan, H. Stormer, P. Kim, Nature **438**, 201 (2005)
2. K.S. Novoselov, A.K. Geim, S.V. Morozov, D. Jiang, M.I. Katsnelson, I.V. Grigorieva, S.V. Dubonos, A.A. Firsov, Nature **438**, 197 (2005)
3. A.K. Geim, K.S. Novoselov, Nat. Mater. **6**, 183 (2007)
4. K.S. Novoselov, A.K. Geim, S.V. Morozov, D. Jiang, Y. Zhang, S.V. Dubonos, I.V. Grigorieva, A.A. Firsov, Science **306**, 666 (2004)
5. A. Reina, X. Jia, J. Ho, H. Son, V. Bulovic, M.S. Dresselhaus, J. Kong, Nano Lett. **9**, 30 (2009)
6. A.N. Obraztsov, E.A. Obraztsova, A.V. Tyurnina, A.A. Zolotukhin, Carbon **45**, 2017 (2007)
7. C. Berger, Z. Song, X. Li, X. Wu, N. Brown, C. Naud, D. Mayou, T. Li, J. Hass, A.N. Marchenkov, E.H. Conrad, P.N. First, W.A. de Heer, Science **312**, 1191 (2006)
8. D.A. Dikin, S. Stankovich, E.J. Zimney, R.D. Piner, G.H.B. Dommett, G. Evmenenko, S.T. Nguyen, R.S. Ruoff, Nature **448**, 457 (2007)
9. X. Li, W. Cai, J.H. An, S.Y. Kim, J.H. Nah, D. Yang, R. Piner, A. Velamakanni, I.H. Jung, E. Tutuc, S.K. Banerjee, L. Colombo, R.S. Ruoff, Science **324**, 1312 (2009)
10. S.J. Chae, F. Günes, K.K. Kim, E.S. Kim, G.H. Han, S.M. Kim, H.J. Shin, S.M. Yoon, J.Y. Choi, M.H. Park, C.W. Yang, D. Pribat, Y.H. Lee, Adv. Mater. **21**, 2328 (2009)
11. S. Bae, H. Kim, Y. Lee, X. Xu, J. Park, Y. Zheng, J. Balakrishnan, T. Lei, H. Kim, Y. Song, Y. Kim, K. Kim, B. Ozyilmaz, J. Ahn, B. Hong, S. Iijima, Nat. Nanotechnol. Published online: 20 June 2010. doi:10.1038/nnano.2010.132
12. C.V. Thompson, Annu. Rev. Mater. Sci **20**, 245 (1990)
13. A.C. Ferrari, J.C. Meyer, V. Scardaci, C. Casiraghi, M. Lazzeri, F. Mauri, S. Piscanec, D. Jiang, K.S. Novoselov, S. Roth, A.K. Geim, Phys. Rev. Lett. **97**, 187401 (2006)
14. A. Gupta, G. Chen, P. Joshi, S. Tadigadapa, P.C. Eklund, Nano Lett. **6**, 2667 (2006)
15. Q. Yu, J. Lian, S. Siriponglert, H. Li, Y.P. Chen, S.S. Pei, Appl. Phys. Lett **93**, 113103 (2008)